



# Photoconductivity kinetics in $\text{AgIn}_5\text{S}_8$ thin films

A.F. Qasrawi<sup>a,b,\*</sup>, T.S. Kayed<sup>a</sup>, İsmail Ercan<sup>c</sup>

<sup>a</sup> Group of Physics, Faculty of Engineering, Atılım University, 06836 Ankara, Turkey

<sup>b</sup> Department of Physics, Arab-American University, Jenin, West Bank, Palestine

<sup>c</sup> Department of Physics, Faculty of Arts and Sciences, Düzce University, 81620 Düzce, Turkey

## ARTICLE INFO

### Article history:

Received 1 July 2010

Received in revised form 7 August 2010

Accepted 13 August 2010

Available online 24 August 2010

### PACS:

73.40.Sx

72.20.Ee

73.61.-r

### Keywords:

Thin films

Vapor deposition

Semiconductors

X-ray diffraction

## ABSTRACT

The temperature ( $T$ ) and illumination intensity ( $F$ ) effects on the photoconductivity of as grown and heat-treated  $\text{AgIn}_5\text{S}_8$  thin films has been investigated. At fixed illumination intensity, in the temperature region of 40–300 K, the photocurrent ( $I_{ph}$ ) of the films was observed to decrease with decreasing temperature. The  $I_{ph}$  of the as grown sample behaved abnormally in the temperature region of 170–180 K. At fixed temperature and variable illumination intensity, the photocurrent of the as grown sample exhibited linear, sublinear and supralinear recombination mechanisms at 300 K and in the regions of 160–260 K and 25–130 K, respectively. This behavior is attributed to the exchange of role between the linear recombination at the surface near room temperature and trapping centers in the film which become dominant as temperature decreases. Annealing the sample at 350 K for 1 h improved the characteristic curves of  $I_{ph}$ . The abnormality disappeared and the  $I_{ph} - T$  dependence is systematic. The data analysis of which revealed two recombination centers located at 66 and 16 meV. In addition, the sublinear recombination mechanism disappeared and the heat-treated films exhibited supralinear recombination in most of the studied temperature range.

© 2010 Elsevier B.V. All rights reserved.

## 1. Introduction

$\text{AgIn}_5\text{S}_8$  thin films are attracting considerable attention [1–8] due to their technological applications. It has been shown that the photosensitive  $\text{AgIn}_5\text{S}_8/(\text{InSe}, \text{GaSe})$  heterojunctions can be fabricated using bulk crystals grown from the melt and from the vapor phase or polycrystalline thin films of the ternary compound. These junctions could be used as selective photodetectors [1]. In addition, photovoltaic devices using  $\text{CuI}/\text{AgIn}_5\text{S}_8$  have been produced [2]. The value of the short circuit current for this device is reported as  $1.5 \text{ mA cm}^{-2}$ . Recently, chemically synthesized Sb-doped p-type  $\text{AgIn}_5\text{S}_8$  films grown on indium–tin–oxide coated glass substrates exhibited a maximum photocurrent density of  $5.02 \text{ mA cm}^{-2}$  under illumination using a 300 W Xe lamp system [9].

In our previous works, we have studied some of the physical properties of the  $\text{AgIn}_5\text{S}_8$  thin films [4,10,11]. Namely, the thin film growth conditions, the as grown film's electrical and optical properties in addition to the post annealing effects at temperatures of 450 K and 600 K on the structural and optical properties of the films has been reported. In the current work, we will study the photocon-

ductivity kinetics in  $\text{AgIn}_5\text{S}_8$  thin films. Particularly, temperature and incident light illumination effects on the photoconductivity of  $\text{AgIn}_5\text{S}_8$  thin films will be investigated and analyzed to obtain the optimum conditions for best photovoltaic properties.

## 2. Experimental details

The lumps of  $\text{AgIn}_5\text{S}_8$  crystals which were used as the evaporation source materials, were placed in quartz ampoule that was wound with molybdenum heating coil and heated to  $1100^\circ\text{C}$  at a pressure of  $10^{-5}$  Torr. The glass substrates ( $19 \text{ mm} \times 24 \text{ mm}$ ) were first cleaned in dilute solution of detergent kept at  $70^\circ\text{C}$  to remove gross dirt and protein material and then it was inserted into a boiling solution of  $\text{H}_2\text{O}_2$  (30%) to convert the organic materials to water soluble compounds. The substrate's cleaning procedure was applied in an ultrasonic cleaner, kept in methanol and were then dried by blowing with dry hot air prior to deposition. The film thickness was determined by an optical interference method and was found to be  $\sim 500 \text{ nm}$ . The average deposition rate was around  $1 \text{ nm/s}$ . Some of the deposited films were subjected to a post annealing procedure at 350 for 1 h under nitrogen atmosphere. The films were evaporated onto glass substrates in Hall-bar, square and Van der Pauw shapes using appropriate masks. Electrical contacts were obtained by the evaporation of indium. The ohmic behavior of the contacts was confirmed by the linear variation of the current–voltage ( $I$ – $V$ ) characteristics which was independent of the reversal of the applied bias.

Cooling of the sample was achieved using a closed cycle cryostat (Advanced Research Systems) and Lake Shore 340 temperature controller. The photocurrent of the samples was recorded at various illumination intensities in the temperature range of 25–300 K. The illumination (from tungsten lamp) intensity was recorded using IL1700 radiometer.

\* Corresponding author at: Atılım University, Electrical and Electronics Engineering, Kizilcasar Koyu, Incek-Golbasi, 06836 Ankara, Turkey.  
Tel.: +90 312 5868329; fax: +90 312 5868091.

E-mail address: [aqasrawi@atilim.edu.tr](mailto:aqasrawi@atilim.edu.tr) (A.F. Qasrawi).

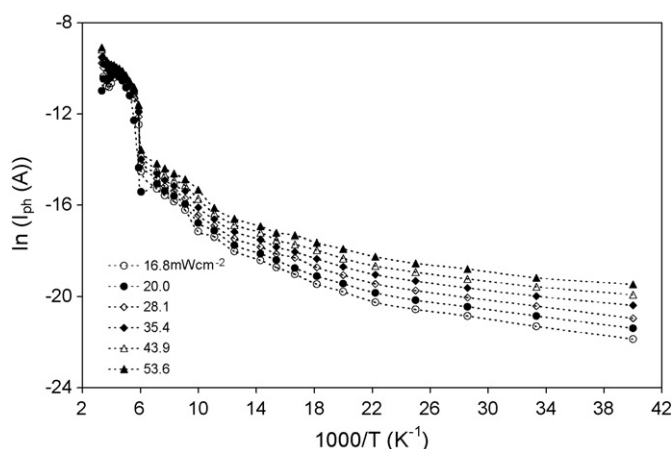


**Fig. 1.** The  $\ln(I_{ph}) - T^{-1}$  dependence at various illumination intensities for the as grown  $\text{AgIn}_5\text{S}_8$  films.

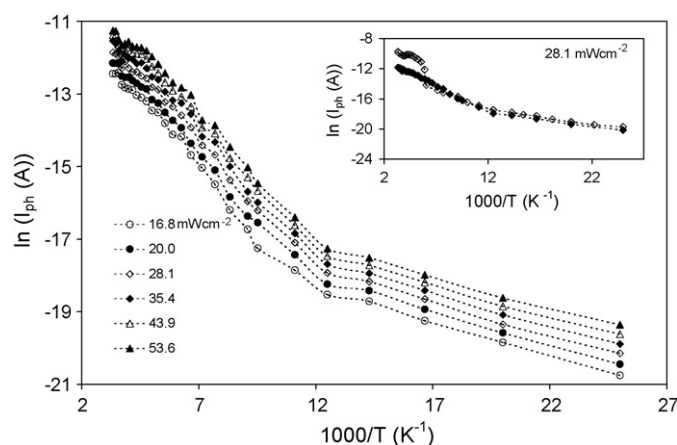


**Fig. 2.** The  $\ln(I_{ph}) - T^{-1}$  dependence at various illumination intensities for the heat-treated  $\text{AgIn}_5\text{S}_8$  films. The inset displays a comparison between as grown and heat-treated samples.

### 3. Results and discussion

The structural, compositional [4] and optical properties [11] of the  $\text{AgIn}_5\text{S}_8$  thin films were previously reported. In that works we have shown that the films are single-phased crystalline  $\text{AgIn}_5\text{S}_8$ . The X-ray data analysis did not show any abnormal peaks. However, because simple heating of  $\text{AgIn}_5\text{S}_8$  in vacuum usually result in decomposition of the compound. Volatile products are expected to be In-rich and Ag-poor. Since one of the crystalline modifications of  $\text{In}_2\text{S}_3$  has the same lattice constant and symmetry [12], so it cannot be distinguished from  $\text{AgIn}_5\text{S}_8$  by XRD only. So, it is very likely that the film consists of S-poor  $\text{In}_2\text{S}_3$  with some dissolved  $\text{Ag}_2\text{S}$ . This possibility was checked and removed by the optical transition spectral analysis reported in Ref. [11]. In that reference we have determined the energy band gap of the  $\text{AgIn}_5\text{S}_8$  as 1.78 eV (coincide with that reported for pure  $\text{AgIn}_5\text{S}_8$  films [3]). This value is less than 2.30 eV and much greater than 1.14 eV which were reported for  $\text{In}_2\text{S}_3$  and  $\text{Ag}_2\text{S}$  thin films, respectively [12,13].

Photoconductivity measurements on the as grown  $\text{AgIn}_5\text{S}_8$  thin films were carried out at different light intensities ( $F$ ) in the intensity range of 16–54  $\text{mW cm}^{-2}$  and temperature region of 25–300 K. The electric field was fixed at 8.4  $\text{V cm}^{-1}$ . The photosensitivity,  $S$ , defined as  $I_{ph}/I_d$ , where  $I_{ph}$  and  $I_d$  are the photo and dark currents, respectively, is found to increase with increasing illumination intensity and decreasing temperature. As for example, the sample have the photosensitivity of 1.2 K, 2.7 K and 5.4 K at 300 K, which increases to  $2.7 \times 10^2$ ,  $6.8 \times 10^2$ , and  $3.0 \times 10^3$  at 25 K, for an applied illumination intensities of 16.8  $\text{mW cm}^{-2}$ , 28.1  $\text{mW cm}^{-2}$  and 53.6  $\text{mW cm}^{-2}$ , respectively.

Fig. 1 displays the semilogarithmic plot of photocurrent ( $I_{ph}$ ) as function of reciprocal temperature. As it can be seen from the figure, at fixed illumination intensity in the high temperature region (190–300 K) the photocurrent–temperature variation is weak. In that region, increasing the temperature increases the  $I_{ph}$  for  $F \geq 35.4 \text{ mW cm}^{-2}$ . At lower  $F$  values,  $I_{ph}$  increases with increasing temperature up to 250 K, where it then starts decreasing. At  $T = 170$ –180 K, the photocurrent of the as grown sample exhibits a very sharp decrease regardless of the light intensity value. In the temperature region of  $25 \leq T \leq 160$  K, at fixed illumination intensity, the  $I_{ph}$  is systematically decreasing with decreasing temperature. On the other hand, in that region, at constant temperature,  $I_{ph}$  increase with increasing  $F$ .

The inset of Fig. 2 represents the photocurrent of the as grown sample before and after being heat treated at 350 K for 1 h in nitrogen atmosphere. As can be observed from the inset of the figure, the fluctuations of the photocurrent above 160 K has disappeared

by heat treatment. Although heat treatment of the sample does not affect the behavior and value of the photocurrent below 160 K, it strongly attenuates the photocurrent at higher temperatures. The data of the temperature and light illumination dependence of photocurrent are displayed in Fig. 2. The figure reflects the systematic variation of photocurrent with reciprocal temperature. Particularly, the  $I_{ph} - T^{-1}$  dependence can be separated into two distinct regions, 100–300 and 90–40 K. As illustrated in Fig. 3(a) and (b), the photocurrent–temperature dependence in these two regions is best represented by the relation,  $I_{ph} \propto \exp(-E_{ph}/kT)$ . The plots of  $\ln(I_{ph}) - T^{-1}$  shown in Fig. 3, reflects parallel solid lines that represent activation energy,  $E_{ph}$ , value of 66 meV in the temperature region of 100–250 K. When the slopes of the solid lines are determined in the temperature region of 100–300 K, the photoconductivity activation energy is 61 meV. In the low temperature region 40–90 K, (displayed in Fig. 3(b)) the photoconductivity activation energy is 16 meV. The parallel solid lines in Fig. 3 indicate that the photoconductivity activation energies are the same for all applied illumination intensities. In other words, the  $E_{ph}$  values do not depend on illumination intensity.

Previously we have determined the dark conductivity activation energy as 221 meV and 147 meV for the as grown sample [4]. The heat treatment at 350 K, reduces the dark conductivity activation energies to 150 meV and 78 meV, respectively. This reduction of resistivity values is mainly attributed to the improved crystalline nature of the films by annealing [11]. The photoconductivity activation energy values being 66 meV and 16 meV are different from that we have found for the dark conductivity measurements. This result indicates that the photocurrent originates from energy states that are detectable only under light excitation and can be regarded as recombination centers.

Fig. 4 illustrates the typical representation of the photocurrent growth as a function of illumination intensity at different temperatures for the heat-treated sample. As it is evident from the figure,  $I_{ph} \propto F^\gamma$ . Generally,  $\gamma$  is observed to vary upon temperature change. The variation of  $\gamma$  with temperature is displayed in Fig. 5. As shown in this figure, for the as grown sample  $\gamma$  sharply decreases from a value of  $\sim 1.0$  at 300 K to a value of 0.31 at 190 K. Below 190 K,  $\gamma$  sharply increases with decreasing temperature exhibiting values greater than 1.0 below 130 K. On the other hand, the heat-treated sample exhibited  $\gamma$  values greater than one at almost all temperatures.

The values of  $\gamma = 1.0$ ,  $\gamma = 0.5$  and  $\gamma > 1.0$  reflect the domination of linear, sublinear and supralinear recombination mechanisms in  $\text{AgIn}_5\text{S}_8$  thin films. The observation of  $\gamma$  between 0.31 and 1.0 may

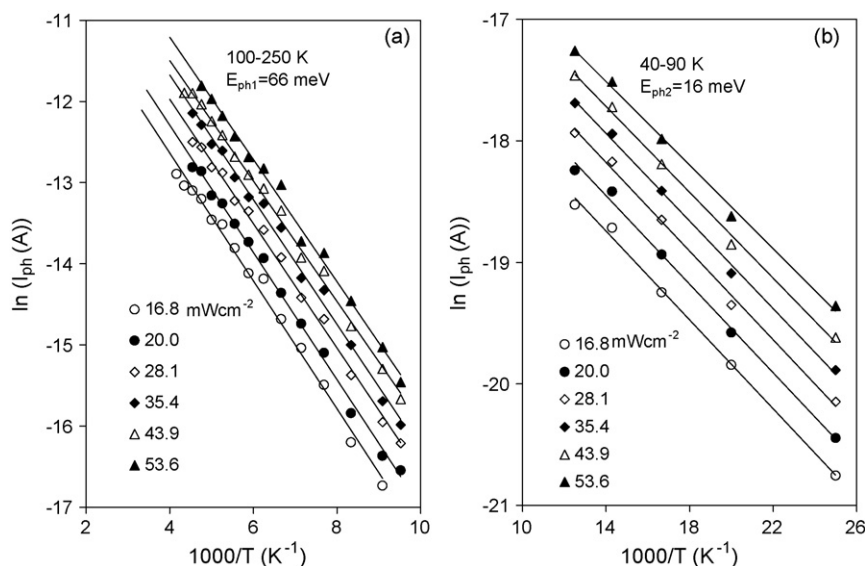


Fig. 3. The  $\ln(I_{ph}) - T^{-1}$  dependence in the temperature range of (a) 100–250 K and (b) 90–40 K.

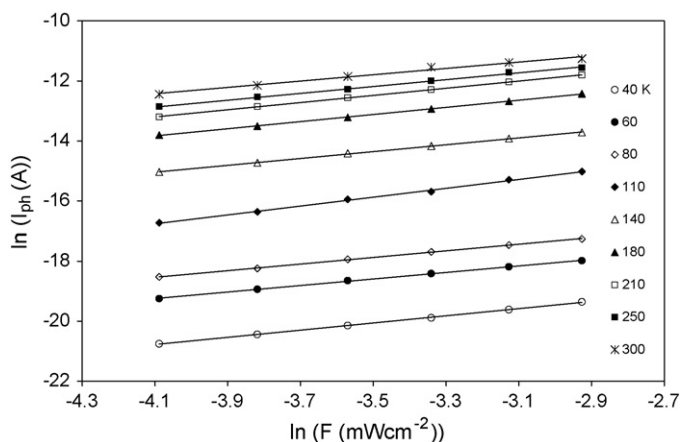


Fig. 4. The illumination intensity–photocurrent dependence at various temperatures for the heat-treated sample.

be explained by considering the presence of band tail with exponential distribution of density of states being distributed in the band gap of the as grown film. The idea was originally proposed by Rose [14,15]. The exponential electron trap distribution is given

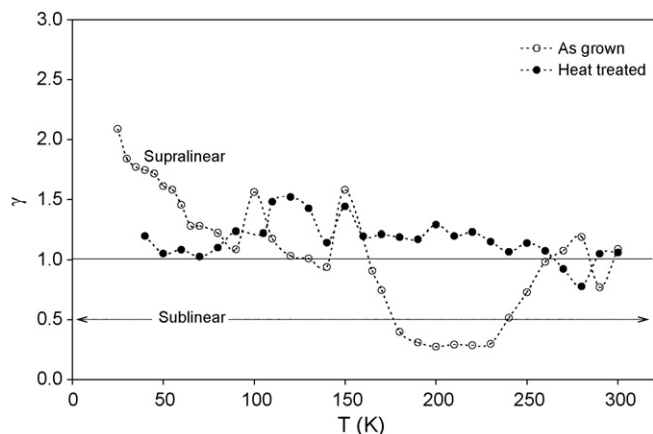


Fig. 5. The exponent  $\gamma - T$  dependence for the as grown and heat-treated samples.

as,

$$n_t = A \exp\left(-\frac{E_c - E_t}{kT^*}\right) \quad (1)$$

where  $A$  is the pre-exponential factor,  $E_c - E_t$  represents the trap distribution location from the conduction band-edge and  $T^*$  is the characteristic temperature which can be adjusted to make the density of states vary more or less rapidly with energy. According to Rose, the exponent in the relation  $I_{ph} \propto F^\gamma$  is given by,

$$\gamma = \left(\frac{T^*}{T + T^*}\right) \quad (2)$$

such that for:  $T^* = T$ ,  $\gamma \rightarrow 0.5$ ;  $T^* \ll T$ ,  $\gamma \rightarrow 0$  and  $T^* \gg T$ ,  $\gamma \rightarrow 1.0$ . For  $\gamma \rightarrow 0.5$ , the trap density is gathered close to the band-edge, corresponding to shallow states, whereas for  $\gamma \rightarrow 1.0$ , the trap states extend close to the middle of the gap, corresponding to deep levels. As the light intensity is increased, more and more of the  $n_t$  states are converted from trapping states to recombination states [15]. This conversion occurs as the Fermi-level penetrates through the  $n_t$  states toward the conduction band.

The data displayed in Fig. 1, has shown a sharp transition in the photocurrent values around 180 K. This thermal transition is associated with a transition from sublinear to supralinear recombination mechanism as in Fig. 5. The observation of a supralinear photocurrent ( $\gamma > 1.0$ ) at fixed temperature and thermal quenching of photocurrent at fixed illumination intensity may then be attributed to exchange in the behavior of the sensitizing centers. In other words, the supralinear character at fixed temperature is observed when sensitizing centers change their behavior from traps to recombination centers. On the other hand, when sensitizing centers change their behavior from recombination centers to traps at fixed illumination intensity, thermal quenching of photocurrent is observed [16].

In attempt to explain the kinetics of the photoconductivity, it is worth notifying that both sublinear recombination and trapping effect in addition to photocurrent sharp transition in the range of 170–180 K has disappeared when the sample was heat treated at 350 K. Consistently Fig. 5 reflects the domination of supralinear recombination for the heat-treated sample. These significant changes suggest that the heat treatment has reduced the density of the trapping centers. Recalling that the dark resistivity values for both as grown and heat-treated samples increases with decreasing temperature, then the photoconductivity is most probably affected

by the location of the dark Fermi-level. In other words, as suggested by Misra and Moustakas [15], for low resistivity values at high temperatures, the dark Fermi-level lies close to the conduction band. Under light, the quasi-Fermi-level sweeps through only a small range of energies towards the conduction band. Thus, the number of previously empty trap states that are converted to recombination states is relatively small which makes the trap state effect apparent. In addition, states closer to the band-edge are less efficient as recombination centers. Therefore, the electron lifetimes are long. The observation that  $\gamma$  is sublinear suggests that the concentration of band-tail states close to the conduction band-edge is large. The interaction of these trap states with the conduction band is evidenced in the slow component of the time response. For high resistivity values at low temperatures, the dark Fermi-level lies deeper in the band gap. On illumination, the quasi-Fermi-level moves closer to the conduction band, sweeping through a larger band of energy. The number of previously empty trap states that are converted to electron recombination states is larger. Being closer to the middle of the gap, these states are more efficient recombination centers, yielding shorter lifetimes for the electrons. Thus, supralinear recombination appears. The fact that recombination is linear suggests that the distribution of the band-tail states is more uniform, leading to a smaller density of trap states close to the conduction band-edge. Thus, the effect of trapping on the response time is weak [15,16].

#### 4. Conclusions

In this work, the photoelectrical properties of the as grown and heat-treated  $\text{AgIn}_5\text{S}_8$  thin films were investigated. The photoconductivity kinetics has been studied by means of illumination and temperature dependencies of the photocurrent. Particularly, at fixed illumination intensity, the photocurrent is observed to decrease with decreasing temperature. Such behavior is ascribed to the conversion of trapping levels to recombination centers

which is associated with recombination center shift from deep to shallow levels. On the other hand, for the as grown sample, the photoconductivity–illumination intensity dependence converts from linear to sublinear and to supralinear recombination as temperature decreases. The heat-treated sample does not reflect sublinear but mostly supralinear recombination mechanism.

#### Acknowledgements

The author thanks Prof. Dr. N.M. Gasanly for the source material supporting and for the unlimited constructive help during this work. Many thanks to Prof. Dr. I. Günel for the technical support during the film preparation process.

#### References

- [1] I.V. Bondar, V.F. Gremenok, V.Yu. Rud, Yu.V. Rud, *Semiconductors* 33 (1999) 740–743.
- [2] I. Konovalov, L. Makhova, R. Hesse, R. Szargan, *Thin Solid films* 493 (2005) 282–287.
- [3] I.V. Bodnar, V.F. Gremenok, *Thin Solid Films* 487 (2005) 31–34.
- [4] A.F. Qasrawi, T.S. Kayed, I. Ercan, *Mater. Sci. Eng. (B)* 113 (2004) 73–78.
- [5] L.V. Makhova, I. Konovalov, R. Szargan, *Phys. Status Solidi (a)* 201 (2004) 308–311.
- [6] M. Gorska, R. Beaulieu, J.J. Loferski, B. Roessler, *Thin Solid Films* 67 (1980) 341.
- [7] A.F. Qasrawi, N.M. Gasanly, *Cryst. Res. Technol.* 36 (2001) 457–464.
- [8] N.S. Orlova, I.V. Bondar, E.A. Kudritskaya, *Cryst. Res. Technol.* 33 (1998) 37–42.
- [9] Cheng, Kong-Wei, Huang, Chao-Ming, Pan, Guan-Ting, Chang, Wen-Sheng, Lee, Tai-Chou, Yang, Thomas C.K., *Phys. B: Condens. Matter* 404 (2009) 1264–1270.
- [10] A.F. Qasrawi, *Thin Solid Films* 516 (2008) 1116–1119.
- [11] A.F. Qasrawi, *J. Alloys Compd.* 455 (2008) 295–297.
- [12] T. Asikainen, M. Ritala, M. Leskelä, *Appl. Surf. Sci.* 82–83 (1994) 122–125.
- [13] H. Djal, M. Amlouk, S. Belgacem, P. Girard, D. Barjon, *Eur. Phys. J. Appl. Phys.* 2 (1998) 13–16.
- [14] A. Rose, *Concepts in Photoconductivity and Allied Problems*, Interscience Publishers, Singapore, 1963 (Chapter 3, p38).
- [15] M. Misra, T.D. Moustakas, *Mater. Res. Soc. Symp.* 622 (2000) (T5. 4. 1).
- [16] R.H. Bube, *Photoelectronic Properties of Semiconductors*, Cambridge University Press, Cambridge, 1992, p72.